# What do accumulation records of single ice cores in Greenland represent?

Traute Crüger
Institute for Coastal Research, GKSS Research Centre, Geesthacht, Germany

Hubertus Fischer
Alfred Wegener Institute for Polar and Marine Research (AWI), Bremerhaven, Germany

Hans von Storch
Institute for Coastal Research, GKSS Research Centre, Geesthacht, Germany

Received 14 May 2004; revised 12 August 2004; accepted 8 September 2004; published 6 November 2004.

[1] It is investigated to what extent multiannual accumulation time series from Greenland reflect dynamic and thermodynamic processes and how representative single accumulation series are for the entire ice sheet. Furthermore, it is examined whether accumulation is related to low-level atmospheric temperatures. For this purpose, two kinds of regression models are developed which linearly relate multiannual accumulation records to meteorological mean fields. Seven ice cores from north to central Greenland and the NCEP Reanalysis data are used for the period from 1948 to 1992. In order to reduce noise, the data are smoothed with a weighted 5-year running mean. The downscaling technique is based on a stepwise multiple linear regression. One group of regression models distinguishes between dynamic and thermodynamic atmospheric effects. For that reason, stream functions are used in a first step to describe the dynamically controlled accumulation, whereas the thermodynamically controlled accumulation is determined by temperature in a second step. For six of the ice cores, these regression models describe more than 56% of the variability of the smoothed accumulation series, confirming that they represent to a large extent atmospheric states. Multiannual accumulation variability is found to dominantly represent circulation variability. However, the circulation fields that are linked with accumulation show marked differences among the cores concerning the represented seasons, areas, and structures. Thus local accumulation generally represents only regional-scale climate features, which are probably to a great extent influenced by orography. Furthermore, regression models using only 700 hPa temperature as predictor show that a general linear relationship between accumulation and temperature does not exist over this 45-year time interval. Therefore paleoaccumulation rates derived from isotopic temperatures should be interpreted with caution. Moreover, it is not reasonable to describe accumulation by means of temperature in mass balance models for the Greenland ice sheet in decadal timescales. *INDEX TERMS:* 1827 Hydrology: Glaciology (1863); 1863 Hydrology: Snow and ice (1827); 1854 Hydrology: Precipitation (3354); 3344 Meteorology and Atmospheric Dynamics: Paleoclimatology; *KEYWORDS:* ice core accumulation, atmospheric states, downscaling

**Citation:** Crüger, T., H. Fischer, and H. von Storch (2004), What do accumulation records of single ice cores in Greenland represent?, *J. Geophys. Res.*, *109*, D21110, doi:10.1029/2004JD005014.

## 1. Introduction

[2] For the investigation of climate on socially relevant timescales, analyses of decadal variability using long-term data are needed. Since reliable instrumental data are only available for about the last 100 years, paleoclimatic proxy data, such as ice cores, tree-rings and corals, have become a fundamental source of climate information [*Dansgaard et al.*, 1989; *Dahl-Jensen et al.*, 1993; *Briffa et al.*, 2004; *Gagan et al.*, 2000]. Since in the high interior parts of the polar ice sheets melting has not occurred, the snow accumulates over long times and preserves climate features into the present. In order to obtain information from these climate archives, ice cores have been drilled and analysed, mainly from the Greenland and Antarctic ice sheets.

[3] One parameter that can be deduced from ice cores is local snow accumulation. Besides being a fundamental

Copyright 2004 by the American Geophysical Union.
0148-0227/04/2004JD005014$09.00

parameter for the mass balance of the ice sheet [*Ohmura et al.*, 1996, 1999; *van der Veen and Bolzan*, 1999; *McConnell et al.*, 2000a, 2000b; *Wild and Ohmura*, 2000; *Bales et al.*, 2001; *van de Wal et al.*, 2001], accumulation is the most direct indicator for climate or atmospheric parameters because it is closely linked to precipitation [*Ohmura and Reeh*, 1991; *Bromwich and Robasky*, 1993]. Temperature has been indirectly derived from ice cores: the ratio of stable isotopes in precipitation was found to be spatially correlated with local surface temperature [*Dansgaard*, 1953, 1964]. The empirically derived spatial gradient between isotopes and surface temperature was utilized as a temporal gradient in order to estimate past temperatures from ice cores. This "paleothermometer" has often been applied to ice cores in order to estimate past temperatures [*Dahl-Jensen and Johnsen*, 1986; *Dansgaard et al.*, 1989; *Johnsen et al.*, 1992; *GRIP Members*, 1993; *Petit et al.*, 1999]. However, more recent isotope-independent temperature measurements based on borehole thermometry show discrepancies with isotopically derived temperatures [*Cuffey et al.*, 1995; *Dahl-Jensen et al.*, 1998; *Johnsen et al.*, 1995]. *Werner et al.* [2000] suggested from Atmosphere General Circulation Model simulations that this is probably due to a change of the seasonality of precipitation, which leads to systematic changes of the temporal isotope-temperature relationship.

[4] A comparison of isotope-derived temperatures and accumulation rates partly yields a linear relationship between both records. Thus it has been inferred that accumulation is thermodynamically driven [*Dahl-Jensen et al.*, 1993]. However, others [*Alley et al.*, 1993; *Kapsner et al.*, 1995] found contradictions when they tried to explain accumulation only by temperature and suggested that atmospheric circulation changes could have had a greater impact on ice accumulation than temperature. *Crüger and von Storch* [2002] developed a method to determine the extent to which the accumulation is thermodynamically or dynamically controlled. They showed for one north Greenland ice core that the proportion of accumulation variability, which can be described dynamically, dominates the thermodynamically described contributions. In this work, the results of *Crüger and von Storch* [2002] are extended to other ice cores drilled in north, west and central Greenland. It shall be investigated, to what extent accumulation series are determined by the atmosphere's dynamic and/or thermodynamics. Special attention is paid to the question of whether different ice cores reflect similar atmospheric states and thus to the question of how representative single ice cores are. For this reason, for each single ice core a regression model is developed, that relates local accumulation to large-scale meteorological fields, representing separate dynamic and thermodynamic contributions.

[5] Despite the questionable temporal relationship between accumulation and near-surface temperature, temperature has often been considered as a proxy for accumulation. Especially in mass balance models, a positive correlation has been applied to simulate the future evolution of the Greenland ice sheet [*Huybrechts and de Wolde*, 1998; *Greve*, 2000; *van de Wal et al.*, 2001]. *Crüger and von Storch* [2002] directly investigated the relationship between accumulation and atmospheric temperature without using an empirically derived relationship between isotopes and temperature. They found for one ice core from north Greenland that a negative correlation between accumulation and 700 hPa temperature over the entire ice sheet exists for the period between 1948 and 1992. In this work, the relationship between accumulation and temperature is further examined by developing a second group of regression models for local accumulation that only uses 700 hPa temperature fields as a predictor. Here we search for a linear relationship between accumulation and temperature, instead of an exponential link according to Clausius-Clapeyron. Hence, the question shall be investigated, whether a generally valid relationship exists between accumulation and atmospheric temperature.

[6] In section 2 we present the data, which were used for our investigation, before the general procedure to develop the regression models is described (section 3). In section 4 we present the two kinds of regression models for each accumulation series: one distinguishes between the physical processes of dynamics and thermodynamics, the other explains accumulation only be means of temperature. The results are discussed in section 5.

## 2. Data

### 2.1. Ice Core Accumulation

[7] The Alfred Wegener Institute for Polar and Marine Research (AWI) in Bremerhaven (Germany) performed a North Greenland Traverse (NGT) between 1993 and 1995. Many ice and firn cores from north and north central Greenland were obtained and have been evaluated [*Fischer*, 1997; *Hausbrand*, 1998; *Schwager*, 2000; *Sommer*, 1996]. In this paper, we refer to the yearly accumulation time series of five ice cores drilled during the NGT. One of these cores, B21, has been used by *Crüger and von Storch* [2002] in their first attempts building regression models (see above). Furthermore, the accumulation rates of the GISP2 core drilled near Summit [*Cuffey et al.*, 1995; *Cuffey and Clow*, 1997] and the NASA-U core from West Greenland are examined [*Anklin et al.*, 1998; *Appenzeller et al.*, 1998b] (Table 1 and Figure 1). The overlapping period with the atmospheric data (see below) is from 1948 to 1992 for the NASA-U and the AWI cores and for GISP2 from 1948 to 1987. B21 and B18 were drilled in the northeastern outflow region of Greenland, where annual precipitation and accumulation are the smallest of the ice sheet. The highest accumulation rates are found for NASA-U, drilled on the western edge of the ice sheet [*Ohmura et al.*, 1999; *Bales et al.*, 2001; *Dethloff et al.*, 2002].

[8] The annual accumulation rates of the AWI cores and GISP2 have been calculated from measured annual thicknesses and density profiles. The dating of the thicknesses has been performed in two steps: for a first rough dating, volcanic eruption signals have been identified. Additionally, the annual layers have been specified using seasonal varying physical and chemical parameters in the ice [*Meese et al.*, 1994; *Sommer*, 1996; *Fischer*, 1997; *Hausbrand*, 1998; *Schwager*, 2000]. For the period considered here, a maximum dating error of ±2 years is assumed. For NASA-U, the accumulation rates were also calculated from physical or chemical parameters that exhibit seasonal variations. No dating uncertainty can be expected for this record [*Anklin et al.*, 1998]. Some of the cores were drilled on the top of ice divides. Thus it could be more difficult to find relationships

**Table 1.** Coordinates, Elevation, and Annual Mean Accumulation Rates of the Ice Cores for the Period of 1645–1994

| Ice Core | Latitude/ Longitude, °N/°W | Elevation, m | Accumulation, mm $yr^{-1}$ |
|---|---|---|---|
| B21 | 80.0/41.1 | 2185 | 100 |
| B26 | 77.3/49.2 | 2598 | 160 |
| B18 | 76.6/36.4 | 2508 | 104 |
| B29 | 76.0/43.5 | 2874 | 147 |
| B16 | 73.9/37.6 | 3040 | 123 |
| NASA-U | 73.8/49.5 | 2370 | 343[a] |
| GISP2 | 72.6/38.5 | 3200 | 230[b] |

[a]Overlapping period with the atmospheric data: 1948–1992 [*Anklin et al.*, 1998].
[b]Overlapping period with the atmospheric data: 1948–1987 [*Schwager*, 2000].

between atmospheric fields and ice cores from these locations, because the drilling site can directly be influenced from all directions.

[9] There are several sources of noise that potentially affect ice accumulation time series. On the one hand, noise is produced by postdepositional processes such as snow-drift by wind or ice flow in deeper layers. In accumulation time series, this noise primarily influences the high frequencies [*Fisher et al.*, 1985]. Additional noise arises from errors in separating the annual layers in an ice core. An overestimation of accumulation in one year mostly leads to an underestimation in the preceding or following year. Both kinds of noise can be reduced by a smoothing procedure over several time steps [*Fisher et al.*, 1985, 1996; *Appenzeller et al.*, 1998a, 1998b]. Therefore a weighted 5-year running mean (with weights $\frac{1}{9} - \frac{2}{9} - \frac{3}{9} - \frac{2}{9} - \frac{1}{9}$) was applied to the accumulation time series. However, this procedure also reduces the high frequency, i.e. the interannual variability. Therefore the found relationships between accumulation and atmospheric fields mainly describe the multiannual variability.

[10] A more serious problem arises when too many or too few annual layers are detected. This kind of error possibly influences a whole period of the time series and can not be substantially reduced by a smoothing procedure. Apart from this constraint, performing the smoothing procedure and assuming that melting does not occur at the drilling sites all year long and that sublimation can be neglected [*Ohmura and Reeh*, 1991; *Bromwich and Robasky*, 1993; *Pomeroy and Jones*, 1996; *Schwager*, 2000], accumulation can be utilized as a measure for precipitation. Precipitation, however, is directly related to meteorological states. Thus accumulation is a suitable predictand for the statistical downscaling of large-scale meteorological fields.

[11] The individual ice accumulation time series behave differently, which becomes apparent from an Empirical Orthogonal Function (EOF) analysis [*von Storch and Zwiers*, 1999, chapter 13]. For this analysis, we normalized and smoothed the accumulation records, in order to avoid dominations of the pattern by series with high variance. The EOF analysis is performed for the period from 1948 to 1987, when all seven records overlap. The explained variance of the first EOF is 29% (Figure 2). Some of the loadings of the EOF pattern have small values, thus these

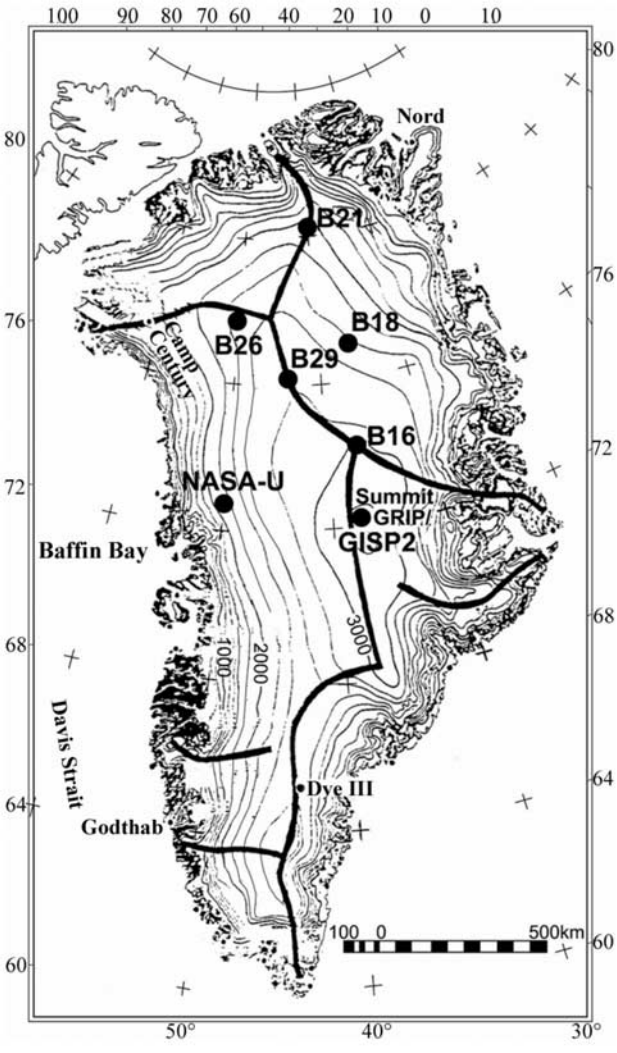


**Figure 1.** Ice core drilling sites, orography, and orographic barriers (thick black lines) in Greenland [*Ohmura and Reeh*, 1991].

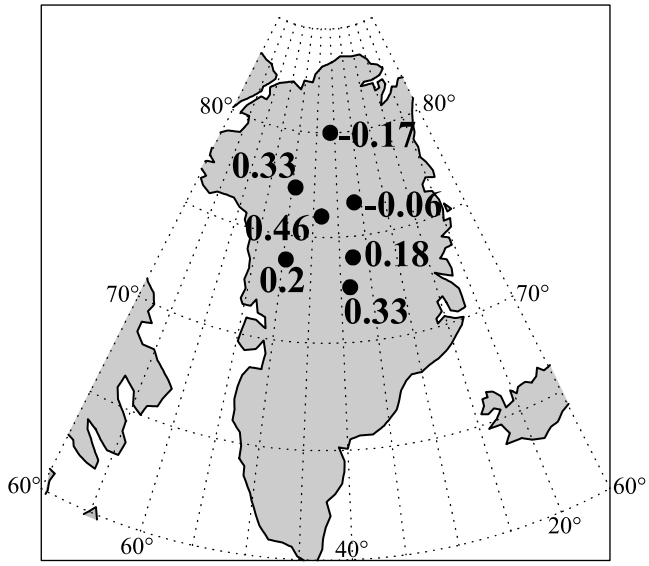


**Figure 2.** First EOF pattern of the normalized and smoothed accumulation records from 1948 to 1987.

series do not have a considerable common signal with the other records, since we used normalized accumulation series for this analysis. Furthermore, both, positive and negative anomalies occur. This sign change has not been found by *Fisher et al.* [1996], who calculated EOFs for Greenland and Canada accumulation series and coastal precipitation records from Greenland and Iceland for a 76-year period. However, they did not involve ice cores from the north and northeastern parts of Greenland. *Kuhns et al.* [1997] investigated 17 shallow ice cores from the Summit region for the period between 1964 and 1983. They found that accumulation records show high coherence in areas smaller than 100 km$^2$. *Clausen et al.* [1988] yield similar results with eight ice cores, some of which representing 360 years. However, the drilling sites of the ice cores used here are farther apart. It is therefore suggested that our accumulation records underly different physical influences. However, it should also be kept in mind that the above mentioned error sources from determining annual layers could also lead to incoherences between the ice cores, influencing the EOFs.

### 2.2. Atmospheric Data

[12] The aim of this work is to find large-scale atmospheric fields that are related to local accumulation. For that reason a fully resolved data set is needed, which has an overlapping period as long as possible with the accumulation time series. Furthermore, the data should realistically represent large-scale atmospheric states. For that reason, we used the 500 hPa velocity and 700 hPa temperature fields of the NCEP Reanalysis data, i.e. the monthly data from 1948 on. Both variables are considered to be reliable [*Kalnay et al.*, 1996; *Kistler et al.*, 2001].

[13] One group of regression models performs a separation between dynamic and thermodynamic contributions to accumulation variability. The dynamic part of these models is solely described by the stream function, which represents the nondivergent part of velocity. In higher latitudes, which are considered in this work, velocity can be assumed to be nearly nondivergent. Thus circulation is well represented by the stream function. A stream function pattern can be interpreted as follows: the direction of the horizontal velocity vector is defined by the tangent at the contour line of stream function. Increasing stream function values are on the right hand side of the flow in the Northern Hemisphere. The velocity is related to the distance between contour lines, small distances indicating high velocity values and vice versa.

[14] Stream function $\psi$ is obtained from the horizontal velocity fields:

$$\nabla^2\psi = \xi = \frac{\partial v}{\partial x} - \frac{\partial u}{\partial y} \tag{1}$$

Here $\nabla^2$ denotes the Laplacian operator and $\xi$ the vorticity. The zonal and meridional wind components are denoted by $u$ and $v$, respectively.

[15] In order to perform an exact calculation of the stream function fields on a sphere, we used the wind components of a Gaussian T21 grid with mean grid distances of about 5.625° × 5.625°. For that reason, firstly the original fields were coarsened from a 2.5° × 2.5° to a 5° × 5° grid by deleting every second row and every second column of the data sets. Afterward, the data were interpolated onto a T21 grid. For a detailed description of the calculation of stream function, see *Washington and Parkinson* [1986].

[16] For the thermodynamically described accumulation, the 700 hPa temperature is used as predictor. For Greenland, this represents the lower atmosphere temperature, which is here used instead of the near-surface temperature, in order to prevent the fields being dominated by local details. For consistency, temperatures were also interpolated onto a Gaussian T21 grid.

[17] Before fitting the regression models, the atmospheric data were temporally smoothed with a weighted 5-year running mean. Thus the same treatment of both, the predictors and the predictands, has been performed.

## 3. Statistical Technique

[18] In the first step of building the dynamic/thermodynamic regression models, we consider only the stream function. A regression model with stream function fields as predictor and ice accumulation as predictand is developed, to identify the dynamically described part of accumulation variability ($A'_{dyn}$).

[19] In the second step, the residual of the real accumulation and the dynamically estimated accumulation is used as the predictand and related to 700 hPa temperature. This part of the model describes the thermodynamically controlled accumulation variability ($A'_{ther}$). By performing this stepwise procedure, temperature, which is related to circulation, is not considered in the second step. The sum of both, $A'_{dyn}$ and $A'_{ther}$, yields the final estimation of accumulation ($A'_{esti}$).

[20] It is possible that the temperature proportion still includes some circulation-related effects, which could not be attributed to stream function. However, we assume that these effects are small, because we intensely searched for dynamic contributions. Thus, if the thermodynamic portion itself is not small, these dynamic effects are considered to be negligible compared to the thermodynamic.

[21] In order to relate large-scale fields to local accumulation, an EOF analysis of the predictors has been performed. This method reduces the time dependencies to only a few time series which are related to fixed patterns containing information on the spatial distribution of the field. The anomalies $G'(x, t)$ of an atmospheric field $G(x, t)$ are expanded into a finite series as follows:

$$G'(x,t) = \sum_{i=1}^{m} g_i(x)a_i(t) + \epsilon_g \tag{2}$$

$g_i(x)$ are fixed patterns (called EOFs) and $a_i(t)$ are time coefficients which are referred to as EOF coefficients or Principal Components (PCs). The residual $\epsilon_g$ is considered to be noise and is neglected in order to develop the regression models.

[22] Then a multiple linear regression is applied which utilises accumulation time series and the PCs of the seasonal mean atmospheric fields. When the PCs of only one predictor are considered, the coefficients of the regression model can be obtained by the following simple formula:

$$k_i = \frac{\sum_{t=1}^{n} a_i(t)A'_{real}(t)}{\sum_{t=1}^{n} (a_i(t))^2} \tag{3}$$

since the PCs of a time series are linearly independent and uncorrelated. Here $k_i$ is the regression coefficient of the $i-$th PC, $A'_{real}(t)$, $t = 1,\ldots, n$ are the anomalies of the local ice accumulation time series. We selected only those $m$ PCs that have a correlation with $A'_{real}(t)$ of more than 0.3. Thus the estimated accumulation anomalies $A'_{dyn}(t)$ is

$$A'_{dyn}(t) = k_1 a_1(t) + \ldots + k_m a_m(t) \quad (4)$$

[23] For the second step described above, this procedure is repeated for 700 hPa temperature. To determine the thermodynamic contribution $A'_{ther}(t)$, we search for high correlations between the predictor PCs and the residual $AR'(t) = A'_{real}(t) - A'_{dyn}(t)$, and in order to calculate the regression coefficients, in equation (3), $A'_{real}(t)$ is replaced by $AR'(t)$. $A'_{ther}(t)$ is obtained by

$$A'_{ther}(t) = r_1 d_1(t) + \ldots + r_l d_l(t) \quad (5)$$

Here the $d_j$(t) are the PCs and $r_j$ the regression coefficients of the second predictor time series.

[24] Regarding the second predictor, the final estimated accumulation ($A'_{esti}(t)$) results from

$$A'_{esti}(t) = A'_{dyn}(t) + A'_{ther}(t) \quad (6)$$

$$A'_{esti}(t) = k_1 a_1(t) + \ldots + k_m a_m(t) + r_1 d_1(t) + \ldots + r_l d_l(t) \quad (7)$$

[25] If the stream function fields of two or more seasons are used in the first step, the PCs are no longer linearly independent, and the regression coefficients can not be calculated according to equation (3). Then a multiple linear regression procedure has been applied using the leading PCs of the different time series [*von Storch and Zwiers*, 1999, chapter 8].

[26] Since EOFs and PCs depend on the spatial boundaries and the averaging period of the field, both the average periods and the field boundaries have been varied in order to maximize the correlation between some of their PCs and the ice core time series. This way the atmospheric fields and their averaging periods and boundaries with the strongest links to accumulation were found [see also *Crüger and von Storch*, 2002].

[27] The second group of regression models are established using 700 hPa temperature as the sole predictor. These models are hereafter referred to as temperature models. In contrast to the dynamic/thermodynamic regression models, the temperature models do not attribute specific physical mechanisms to changes in ice accumulation, because thermodynamic effects as well as dynamic (i.e., circulation-related) temperature effects are included. The temperature-estimated accumulation $A'_{temp}(t)$ is obtained from equation (4), where $A'_{dyn}(t)$ is replaced by $A'_{temp}(t)$ and the $a_i$(t) are the PCs of the temperature fields and the $k_i$ the regression coefficients between temperature PCs and real accumulation.

[28] In order to validate our regression models, a cross-validation method has been used, which has been developed for short time series [*Michaelson*, 1987; *von Storch and Zwiers*, 1999, chapter 18] and has also been used for other paleoclimate reconstructions [*Glueck and Stockton*, 2001; *Jones and Widmann*, 2003]. In this method, a few time steps are removed from the entire time series. The data for the remaining time steps are used to develop a regression model (calculation of seasonal mean anomalies, EOFs and regression coefficients). This model is then applied to predict one of the removed, and therefore independent, time steps. Performing this procedure in a stepwise way means that all time steps are eventually used for validation. Since the fitting and the validation data should be independent, nine time steps are removed from the time series in each step. This is because the running mean procedure is applied over five time steps for the predictand and the predictor series, as explained earlier. The fifth of the nine time steps is the validation time step.

[29] Besides validating our regression models with the cross-validation procedure, we tested our statistical method using several noise time series representing white and red noise [*Jenkins and Watts*, 1968] instead of real accumulation series (accumulation series generally have a white spectrum). The autocorrelation of the time series for the period from 1948 until 1992 (for GISP2 from 1948 until 1987) with a lag of 1 year leads to maximal correlation coefficient of less than 0.3. Therefore we tested our method by using time series of an autoregressive process of order 1 (AR(1)-process) with an AR-coefficient of 0.3 [*von Storch and Zwiers*, 1999, chapter 10]. This way we determined, whether the 'memory' of the time series would lead to an artificial skill of the regression models. For both categories (white noise and AR(1)-process) five time series were produced and the same treatment as for the real accumulation time series were performed. A regression model could not be established for any of these series that describes more than one third of the time series variance. Therefore we claim for our regression models that at least one half of the accumulation variance should be described by the regression model (see below). This way we ensure that the regression models only relate physically reasonable atmospheric fields to the accumulation time series.

## 4. Results

### 4.1. Dynamic/Thermodynamic Regression Models

[30] The components of the dynamic/thermodynamic regression models based on 500 hPa stream function and 700 hPa temperature fields are summarized in Table 2. The table is structured as follows: In the first block the ice core notation appears. The next block includes the features of the stream function components of the regression models. The last block contains the temperature components. In blocks 2 and 3 the first column contains the average period, and the second column contains the spatial extensions of the atmospheric fields. The third and forth columns display the EOF's order and explained variance of the total variance of the atmospheric field. The two last columns show how much variance of the ice accumulation is described for fitting and validation, respectively. The variance always refer to that of the smoothed accumulation series.

[31] For six of the seven ice core records, regression models were obtained with explained variances of more than 56% of the multiannual accumulation variability. For core B26, only about one third of its variability can be

**Table 2.** Components of the Dynamic/Thermodynamic Regression Models[a]

| | Stream Function 500 hPa | | | | | Temperature 700 hPa | | | | | | | Sum of |
|---|---|---|---|---|---|---|---|---|---|---|---|---|---|
| Ice Core | Average Period | Field Boundaries, ° | PC | Expl.Var. of Stream Function | Expl.Var. of Acc. (Fitting) | Expl.Var. of Real Acc. (Validated) | Average Period | Field Boundaries | PC | Expl.Var. Temp. | Expl.Var. of Residual (Fitting) | Expl.Var. of Real Acc. (Validated) | Expl.Var. Ice Acc.(Validated) Streamf.+Temp. |
| B21 | May–Aug. | 68W-51E/ | 1 | 73% | 42% | | annual | 96W-23W/ | 3 | 14% | 21% | | |
| | | 86N-53N | 3 | 6% | 16% | | | 86N-47N | 4 | 9% | 15% | | |
| | | | 4 | 5% | 8% | **64.0%** | | | | | | **7.5%** | 71.5% |
| B26 | Sept.–Nov. | 51W-34E | 1 | 70% | 16% | | | | | | | | |
| | | 86N-53N | 5 | 3% | 33% | **32.1%** | - | - | - | - | - | - | **32.1%** |
| B18 | Sept.–Nov. | 39W-51E/ | 1 | 65% | 9% | | annual | 56W-45E/ | | | | | |
| | | 80N-64N | 3 | 8% | 9% | | | 86N-64N | 2 | 30% | 18% | | |
| | | | 4 | 4% | 44% | **55.5%** | | | | | | **6.5%** | 62.0% |
| B29 | July–Sept. | 96W-79E/ | 1 | 56% | 24% | | annual | 56W-0E/ | 4 | 6% | 22% | | |
| | July–Sept. | 80N-42N | 4 | 7% | 17% | | | 86N-64N | | | | | |
| | Oct.–April | 163W-28W/ | 5 | 3% | 19% | | | | | | | | |
| | | 86N-47N | | | | **45.1%** | | | | | | **12.3%** | 57.4% |
| B16 | May–July | 79W-39E/ | 1 | 61% | 25% | | annual | 39W-23E/ | | | | | |
| | | 80N-42N | 3 | 6% | 33% | **46.7%** | | 86N-53N | 4 | 7% | 19% | **9.4%** | 56.1% |
| GISP2 | Dec.–Feb. | 163W-6E/ | 4 | 7% | 36% | | annual | 62W-22E/ | 4 | 2% | 38% | | |
| | Dec.–Feb. | 86N-53N | 5 | 5% | 17% | | | 75N-64N | | | | | |
| | Sept.–Nov. | 67W-22W/ | 3 | 14% | 19% | | | | | | | | |
| | | 86N-53N | | | | **47.9%** | | | | | | **16.4%** | 64.3% |
| NASA-U | Dec.-Feb. | 79W-73E/ | 3 | 8% | 34% | | annual | 95W-50W/ | | | | | |
| | | 86N-58N | 5 | 2% | 20% | **49.0%** | | 86N-42N | 1 | 45% | 52% | **23.6%** | 72.6% |

[a]Expl.Var., explained variance; Acc., accumulation; Streamf., stream function; Temp., temperature.

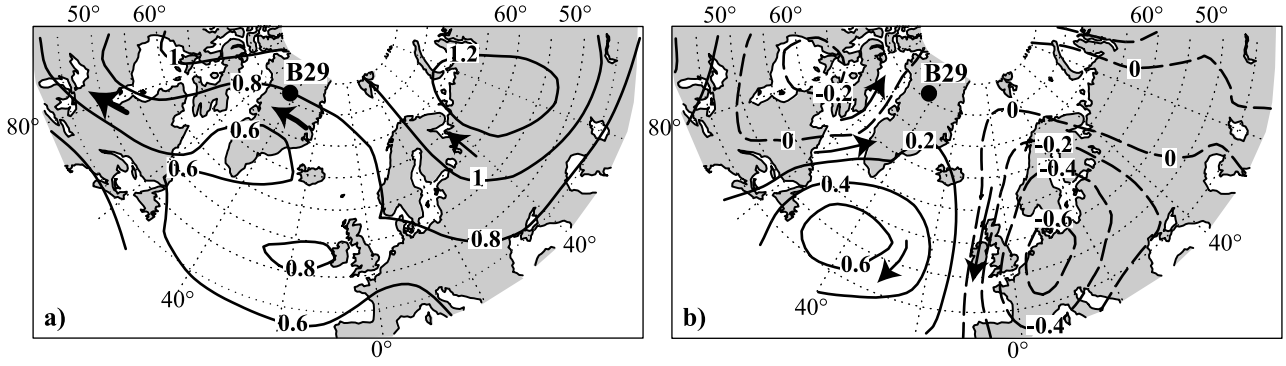


**Figure 3.** B29 dynamic/thermodynamic regression model: EOF pattern of the NCEP 500 hPa stream function (averaged from July to September) (1948 to 1992) [$10^6 m^2 s^{-1}$]; (a) first EOF, (b) fourth EOF.

described. Thus the explained variance for this accumulation record is not higher than for our artificial time series representing white and red noise, respectively (see above). Therefore we assume that B26 is not strongly related to atmospheric states, possibly because of dating errors or local effects, and is not further discussed here.

[32] For all cores the dynamic effects dominate the thermodynamic effects. The dynamic parts of the regression models represent one (B21, B18, B16 and NASA-U) or two (B29 and GISP2) seasonal means, whereas for the thermodynamic parts, annual means have the strongest relationship for all cores. The thermodynamic contributions are small, except for NASA-U, where about two-thirds of the variance of the estimated accumulation is described by circulation and one third by thermodynamics.

[33] The components of the dynamic parts of the regression models are often subordinated EOFs, i.e. normally they do not explain large amounts of variance of the stream function fields. This indicates that the investigated accumulation records mostly are not influenced by dominant atmospheric circulation patterns.

[34] The patterns of the components differ in size and structure between the cores. Also the seasons with the strongest relationships to accumulation differ between the cores. While in the north and northeast the summer and fall contributions dominate, in the west and the central interior of Greenland winter fields tend to explain most of the accumulation variability. Mostly, the average seasons are plausibly related to precipitation: at the site of B21 in North Greenland, precipitation mainly occurs during the summer months [*Chen et al.*, 1997; *Serreze et al.*, 1993; *Ohmura and Reeh*, 1991]. This is in line with the regression model, which relates the accumulation variability to the summer months. For the central parts of Greenland, precipitation is found throughout the year with a maximum in summer [*Ohmura and Reeh*, 1991; *Chen et al.*, 1997; *Serreze et al.*, 1993], and the regression model for B29 indeed considers summer as well as winter contributions. For B16, however, this is not the case. Here the regression model relates almost all accumulation variability to the summer months. Only a small winter contribution is included in the secondary thermodynamic proportion, based on annual means.

[35] For NASA-U, *Appenzeller et al.* [1998b] found a statistically significant correlation between the accumulation and the annual-mean North Atlantic Oscillation (NAO) Index. Our method yields a regression model, whose dynamic part only involves the winter months December to February (DJF). However, correlation maps performed with the sea-level pressure (SLP) from 1900 until 1992 [*Trenberth and Paolino*, 1980] reveal even a stronger NAO-like pattern for DJF than for annual SLP means (not shown), thus supporting the selection of the winter months to explain the NASA-U accumulation variability.

[36] The spatial extensions of the stream function patterns seem to depend on the position of the drilling sites in relation to the ice sheet: B16, B29 and GISP2 are located near the top of the ice sheet. Thus they can directly be influenced from all directions (Figure 1). Stream function patterns have been found, some of which cover an area between the east Pacific Ocean and Eurasia. The other cores, B21, B18 and NASA-U are located at lower elevations. For B18, the patterns seem to directly reflect that the drilling site is screened from the southern and western parts of Greenland by ice divides and mainly cover the area east of B18 (Figure 1). The stream function patterns for B21 and NASA-U cover to a great part the area east of Greenland up to Europe, although both core sites are located west or north of the main ice divide. We assume that the found stream function patterns represent the large-scale circulation, which determines the motion of smaller scale eddies that are not resolved by our stream function data. For NASA-U, it can

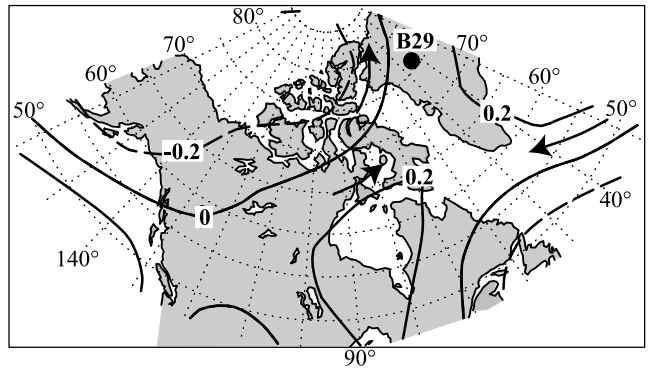


**Figure 4.** B29 dynamic/thermodynamic regression model: fifth EOF pattern of the NCEP 500 hPa stream function (averaged from October to April) (1948 to 1992) [$10^6 m^2 s^{-1}$].

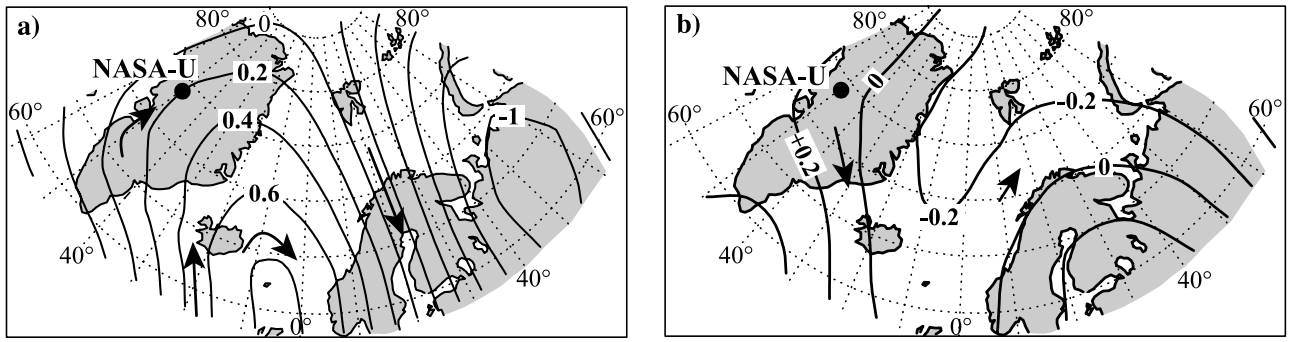


**Figure 5.** NASA-U dynamic/thermodynamic regression model: EOF pattern of the NCEP 500 hPa stream function (averaged from December to February) (1948 to 1992) [$10^6 m^2 s^{-1}$]; (a) third EOF, (b) fifth EOF.

be suggested that the eddies move along the west coast of Greenland, whereas for B21, eddies come from the east.

[37] The structures of the stream function patterns are physically plausible as well, but show marked differences between different cores. We illustrate this by means of the most important patterns of the regression models for B29 and NASA-U. All patterns are shown in the positive phase, i.e. that the shown patterns are accompanied by positive accumulation anomalies, while patterns with an opposite sign are linked with negative anomalies. The arrows show the directions of wind, and their lengths an approximate measure of the wind speed.

[38] For B29, three stream function patterns yield nearly equal contributions to the description of ice accumulation. One summer pattern (Figure 3a) shows that accumulation is influenced by a cyclone located over south Greenland. The other summer pattern and the winter pattern show a westerly flow from the Pacific Ocean and/or North America to Greenland (Figures 3b and 4). This has also been found by *Charles et al.* [1994], who concluded from calculations with a General Circulation Model (GCM) that sources from North America, the North Atlantic and the Pacific Ocean contribute considerably to precipitation in Central Greenland.

[39] For NASA-U, one pattern shows an anticyclonic flow between Iceland and southern Scandinavia. This pattern resembles the northern part of the teleconnection pattern between the monthly SLP and snow accumulation near the drilling site of NASA-U found by *Appenzeller et al.* [1998b] (Figure 5a). The other pattern shows a trough over the Greenland Sea, which is associated with northerly flow at the drilling site (Figure 5b).

[40] Except for NASA-U, the thermodynamic contributions are small: generally, these temperature fields are more confined in extension than the stream function fields and mainly cover Greenland and/or the surrounding areas. As for the stream function patterns, the structure of the temperature patterns widely differ between the cores. In general, they do not relate positive temperature anomalies to positive accumulation anomalies. NASA-U is the only core whose thermodynamic pattern shows a strong temperature maximum near the core site. 23% of the variability of the smoothed accumulation series is explained by thermodynamics. The area of the pattern covers east Canada up to the drilling site (Figure 6). For the other cores, not further discussed here, the patterns of the dynamic/thermodynamic regression models are shown in Figures 10–13.

### 4.2. Temperature Regression Models

[41] The components of the temperature regression models are shown in Table 3, which is structured similar as Table 2. For the cores B21, B18, B29 and NASA-U the derived temperature regression models explain more than 50% of the multiannual accumulation variability, for GISP2 48% (Table 3). The explained variances of the temperature regression models are generally smaller than for the combined dynamic/thermodynamic regression models (Table 2). As for the dynamic/thermodynamic models, marked differences are also found between the temperature regression

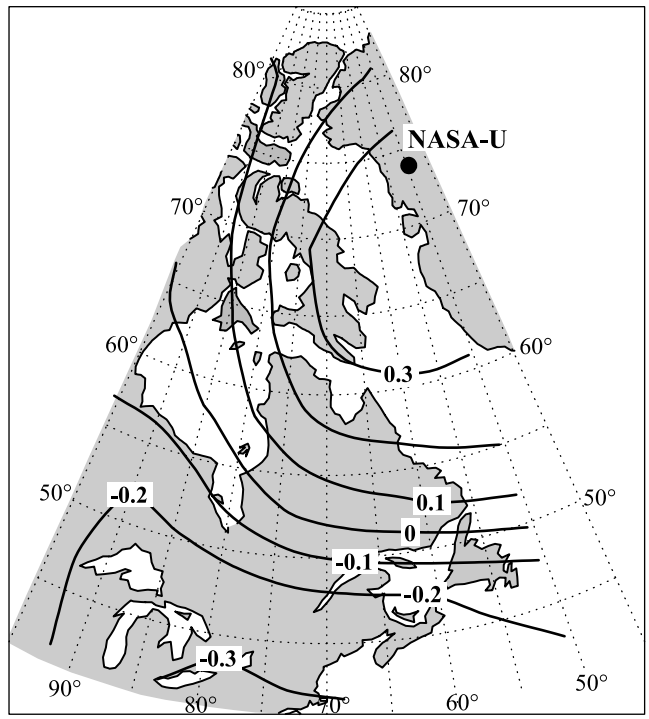


**Figure 6.** NASA-U dynamic/thermodynamic regression model: first EOF pattern of the NCEP 700 hPa annual temperature (1948 to 1992) [°C].

**Table 3.** Components of the Temperature Regression Models[a]

| Annual Temperature 700 hPa | | | | | |
|---|---|---|---|---|---|
| Ice Core | Field Boundaries, ° | Principal Component | Expl.Var. of Temperature Field | Expl.Var. of Ice Acc. (Fitting) | Expl.Var. of Ice Acc. (Validated) |
| B21 | 68W-23W/ | 1 | 73% | 55% | |
| | 86N-64N | | | | **52%** |
| B26 | | | | | **<10%** |
| B18 | 45W-11E/ | 2 | 30% | 57% | |
| | 86N-42N | | | | **56.5%** |
| B29 | 62W-11W/ | 4 | 3% | 52% | |
| | 86N-64N | 3 | 7% | 5% | **51.8%** |
| B16 | 45W-23W/ | 1 | 75% | 27% | |
| | 80N-58N | 4 | 2% | 12% | **22.4%** |
| GISP2 | 62W-28E/ | 4 | 4% | 54% | |
| | 69N-58N | | | | **47.6%** |
| NASA-U | 101W-62W/ | 2 | 33% | 50% | |
| | 63N-47N | 3 | 9% | 9% | **53.3%** |

[a]Expl.Var., explained variance; Ice Acc., ice accumulation.

models for the different cores. This is illustrated by means of the patterns that are linked with B18 and B29 accumulation (Figures 7 and 8). For the other cores, the patterns are shown in Figure 14.

[42] For B18, the pattern that ranges from east Greenland to western Europe, is characterized by negative temperature anomalies over northeast Greenland and especially the European part of the area, while positive temperature anomalies are found south of Greenland (Figure 7).

[43] For B29, the most dominant pattern, essentially covering Greenland, shows slightly negative temperature anomalies near B29 which decrease toward the northwest of the drilling site. In the eastern half of the area, no noteworthy temperature anomalies occur, while temperature anomalies are slightly positive in the south of Greenland (Figure 8). The less important third EOF pattern also relates negative temperature anomalies at the core site to positive ice accumulation anomalies (Figure 14).

[44] B16 is the only investigated ice core whose accumulation time series is positively correlated with NCEP 700 hPa temperature around the drilling site (not shown). However, a regression model that is mainly based on a similar pattern only yields 22.4% explained variance after validation.

### 4.3. Validation

[45] The validated accumulation estimations, here shown for NASA-U, B18 and B29, reveal better results for the dynamic/thermodynamic models than for the temperature-only models, especially for NASA-U. For this core, the dynamic/thermodynamic model (72.6%) explains about 20% more accumulation variability than the temperature

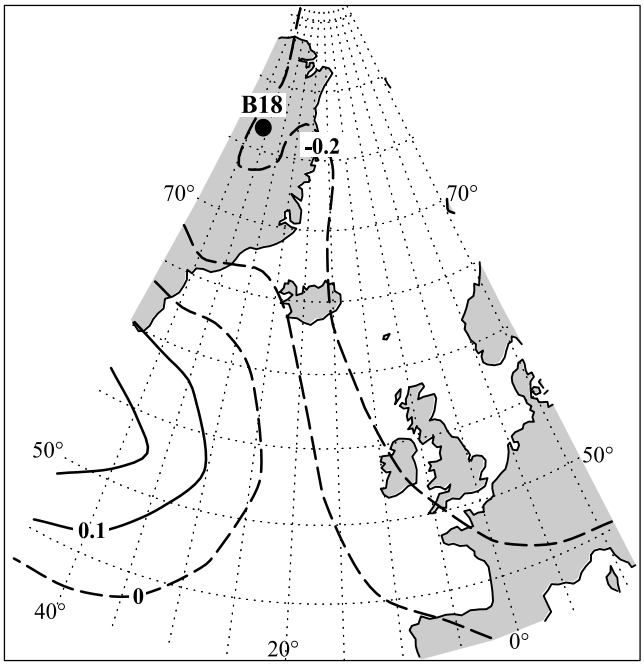


**Figure 7.** B18 temperature regression model: second EOF pattern of the NCEP 700 hPa annual mean temperature (1948 to 1992) [°C].

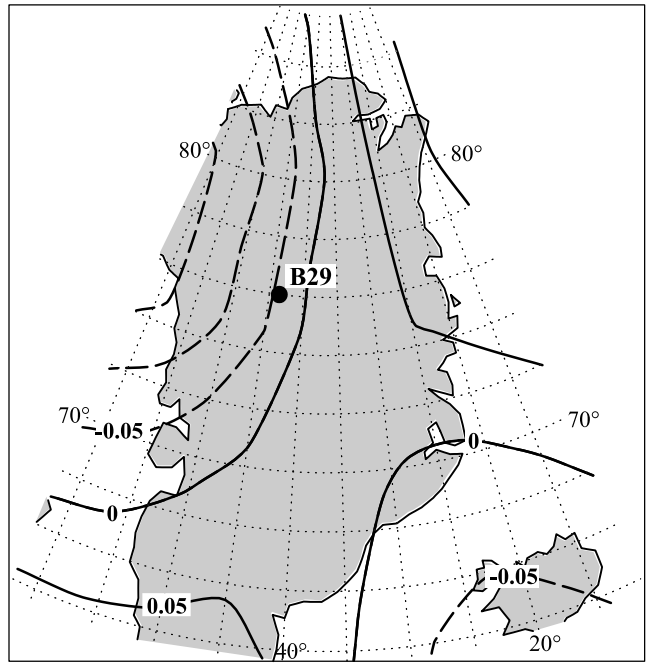


**Figure 8.** B29 temperature regression model: fourth EOF pattern of the NCEP 700 hPa annual mean temperature (1948 to 1992) [°C].

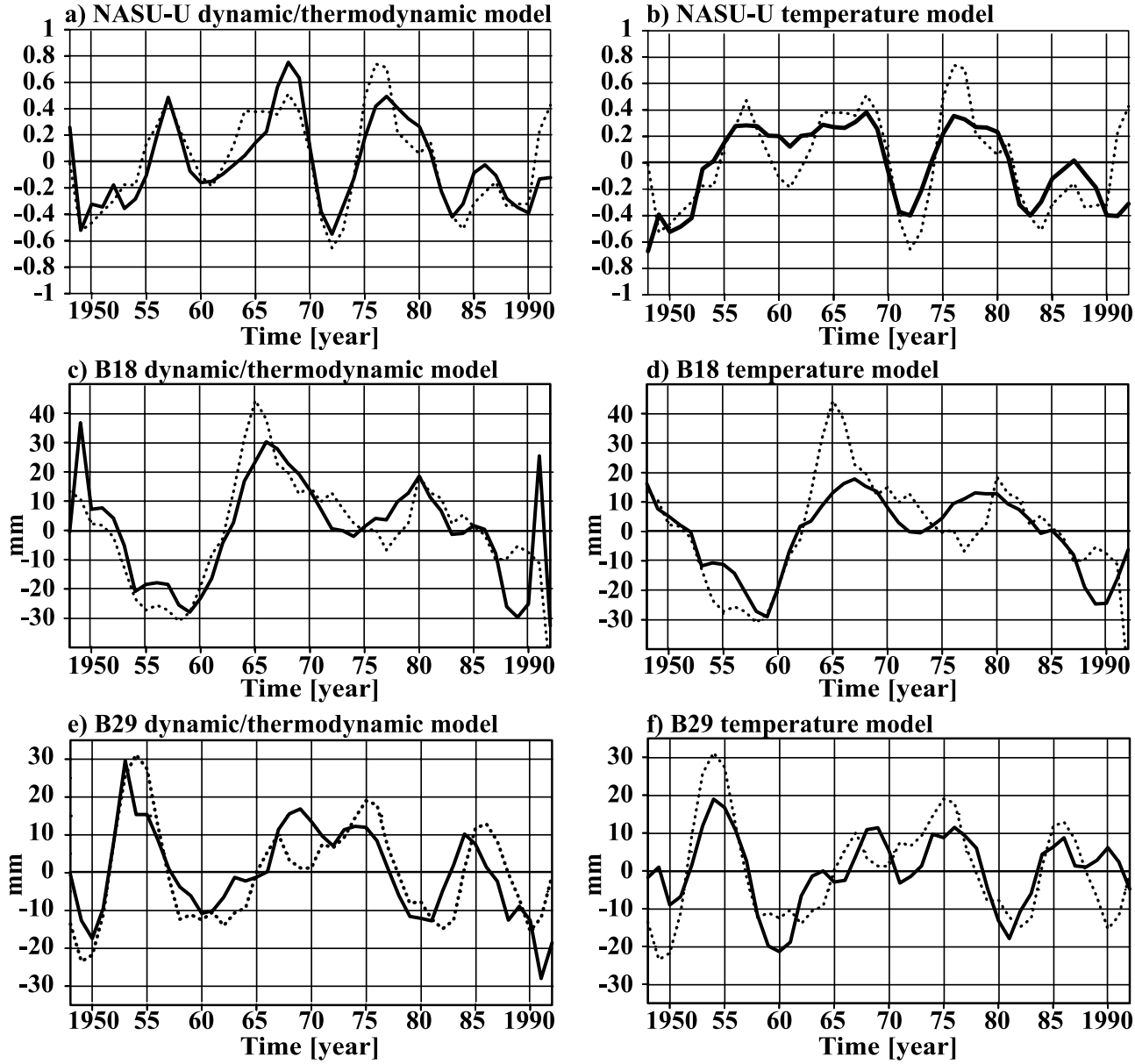


**Figure 9.** Annual accumulation anomalies for NASA-U (top), B18 (middle), and B29 (bottom): cross-validated estimates (solid lines) and observed ice core (dotted lines) for the combined dynamic/thermodynamic model (left) and the temperature-only model (right) (see also Tables 2 and 3).

model (53.3%). All maxima and minima are described by the dynamic/thermodynamic model. This is not the case for the temperature-only model, whose estimation does not match the minimum of 1960 and also leads to poorer estimations from 1970 on (Figures 9a and 9b). B18 is also better described by the dynamic/thermodynamic model during the whole period, except for the second and the penultimate year (Figures 9c and 9d), leading to an explained variance of the dynamic/thermodynamic model of 62.0% instead of 56.5% for the temperature-only model. For B29, the discrepancies between both models are not so obvious. The dynamic/thermodynamic model mainly shows better results for the first two decades (Figures 9e and 9f). The validated estimates for the other cores (not shown) yield similar results, proving that on the whole the physically based dynamic/thermodynamic models (Figures 10–13) lead to better accumulation estimations than the models based only on temperature (Figure 14).

## 5. Discussion

[46] We have shown that it is generally possible to directly describe multiannual accumulation variability by means of large-scale meteorological fields. In order to undertake this investigation, a fully resolved instrumental data set of the atmosphere was needed. Thus our investigation could only involve the relatively short period of 45 years (for GISP2 only 40 years) of the present-day climate, which is probably already anthropogenically influenced. Atmospheric processes or fundamentally different

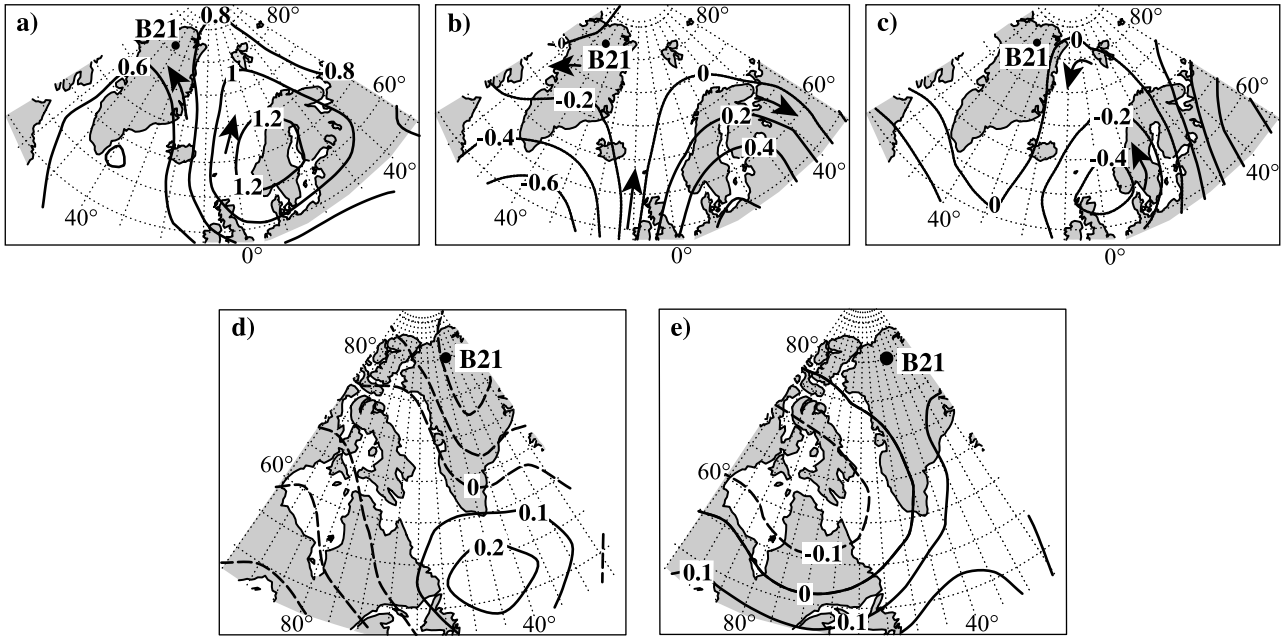


**Figure 10.** B21 dynamic/thermodynamic regression model [*Crüger and von Storch*, 2002]: 500 hPa stream function (May–August) [$10^6 m^2 s^{-1}$] ((a) first EOF, (b) third EOF, (c) fourth EOF); 700 hPa temperature (annual mean) ((d) third EOF, (e) fourth EOF).

circulation patterns, which may have occurred prior to this period, could not be described by the regression models. Furthermore, long-term trends are also not represented by the regression models. Therefore some caution is necessary in applying the results to other climate periods. These constraints should be kept in mind in the further discussion.

[47] Taking into account that there are several error sources and uncertainties which affect the accumulation data, the explained variances of the models are high. However, the explained variances refer to the smoothed accumulation series, whose variance is substantially reduced compared to the variance of the raw accumulation data. The smoothing procedure also causes that interannual variability is not resolved by our regression models. Thus these models do not provide a tool for the reconstruction of interannual atmospheric patterns.

[48] Some core sites are on the top of ice divides and can therefore directly be influenced from all directions. Thus one could expect that for those accumulation series it would be more difficult to find relationships with atmospheric fields. But no considerable difference could be found between the explained variances of the cores from the top of main ice divides and those away from the divides. However, for two of the cores drilled on the top of the

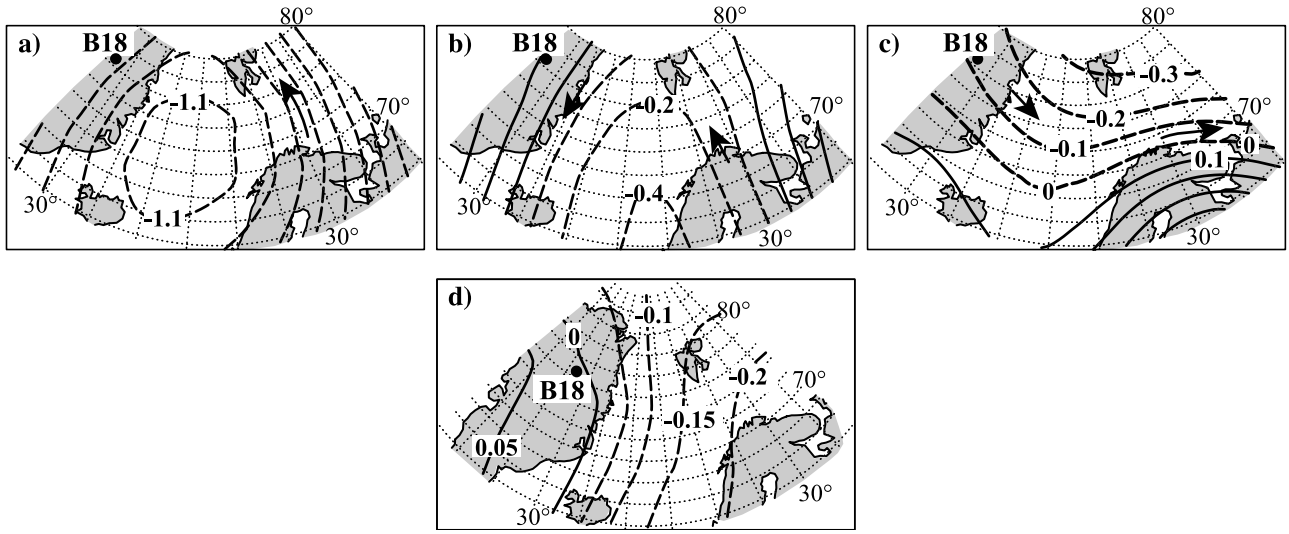


**Figure 11.** B18 dynamic/thermodynamic regression model: 500 hPa stream function (September–November) [$10^6 m^2 s^{-1}$] ((a) first EOF, (b) third EOF, (c) fourth EOF); (d) second EOF of annual mean 700 hPa temperature.

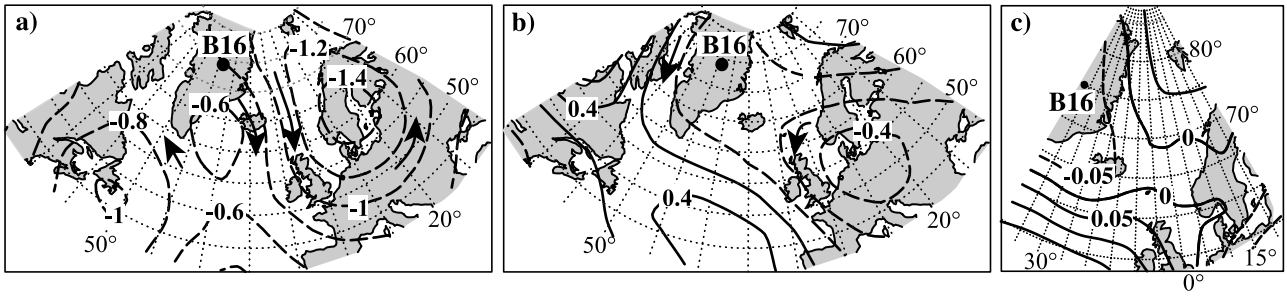


**Figure 12.** B16 dynamic/thermodynamic regression model: 500 hPa stream function (May–July) [$10^6 m^2 s^{-1}$] ((a) first EOF, (b) third EOF); (c) fourth EOF of annual mean 700 hPa temperature.

main ice divide, EOF fields contribute to the description of accumulation, which represent different seasons and areas. Thus our method is capable of attributing influences that represent different temporal and spatial characteristics.

[49] The regression models show that the different behavior of the accumulation records is dominantly due to different physical processes in the atmosphere that influence the different core sites, and not to local noise or some kinds of errors. Thus we can draw some conclusions about the behavior of the multiannual accumulation. There is one dominant common feature, that is found for all ice cores: all accumulation records are mainly controlled dynamically. Thermodynamic contributions remain smaller than the dynamic ones. Thus Greenland's ice accumulation represents mainly circulation. This extends the suggestions made by *Alley et al.* [1993], *Kapsner et al.* [1995], and others that in the Summit area the circulation plays a fundamental role for ice accumulation variability in north Greenland ice cores. Apart from this common feature, the dynamic parts of the regression models show marked differences, indicating different circulation patterns that are linked with ice accumulation variability at the various core sites. These differences suggest that the circulation of Greenland is strongly influenced by local effects, such as the orography. Therefore the flow dynamics over Greenland is not uniform, but highly complex. Since the accumulation of the ice cores investigated here is mainly controlled dynamically, the spatial variability of the ice accumulation is high. As a consequence, the size, position and structures of the stream function regression patterns are a result of the location of the respective drilling site relative to the orographic barriers and ice divides. Thus accumulation commonly represents only regional-scale, but not general large-scale, climate characteristics.

[50] Since local accumulation represents different physical processes of the atmosphere, it seems to be reasonable to investigate ice cores from various sites of Greenland in order to possibly make some inferences. This implies that it is not useful to derive a stacked accumulation record from several time series from well separated locations. The idea, when using a stacked record, is that, besides a common physical signal of the records, there also is a large noise contribution, which is minimized by the stacking procedure. However, we have shown that the smoothed accumulation records represent different physical signals which would have not been found in a stacked ice core combining well separated locations.

[51] Furthermore, it has been investigated, whether regression models can be derived that use 700 hPa temperature as the sole predictor and link positive temperature anomalies to positive ice accumulation anomalies. Such regression models were not found. However, regression

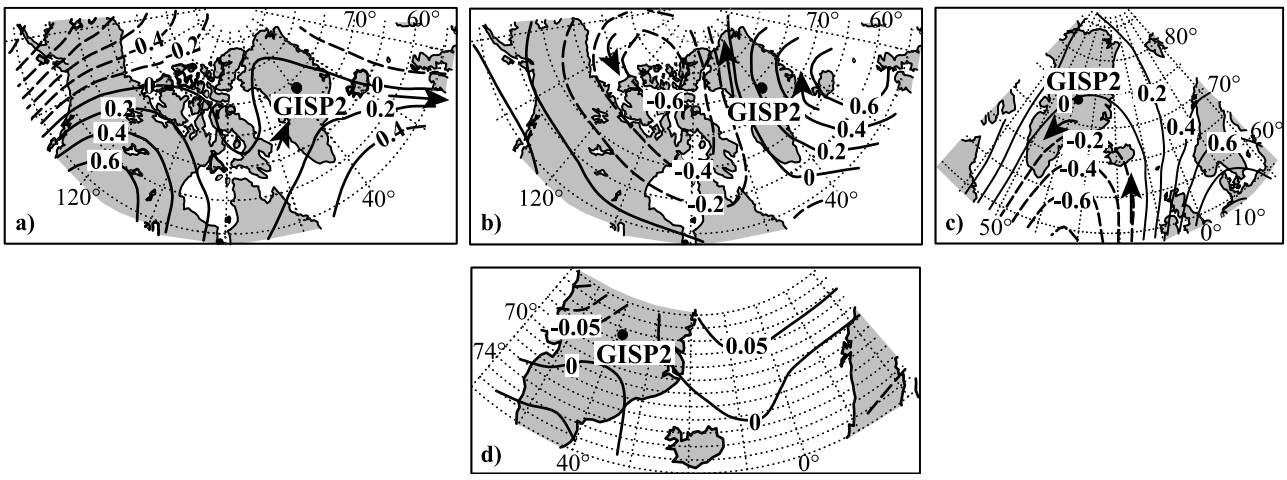


**Figure 13.** GISP2 dynamic/thermodynamic regression model: 500 hPa stream function [$10^6 m^2 s^{-1}$] ((a) fourth EOF (December–February), (b) fifth EOF (December–February), (c) third EOF (September–November)); (d) fourth EOF of annual mean 700 hPa temperature.

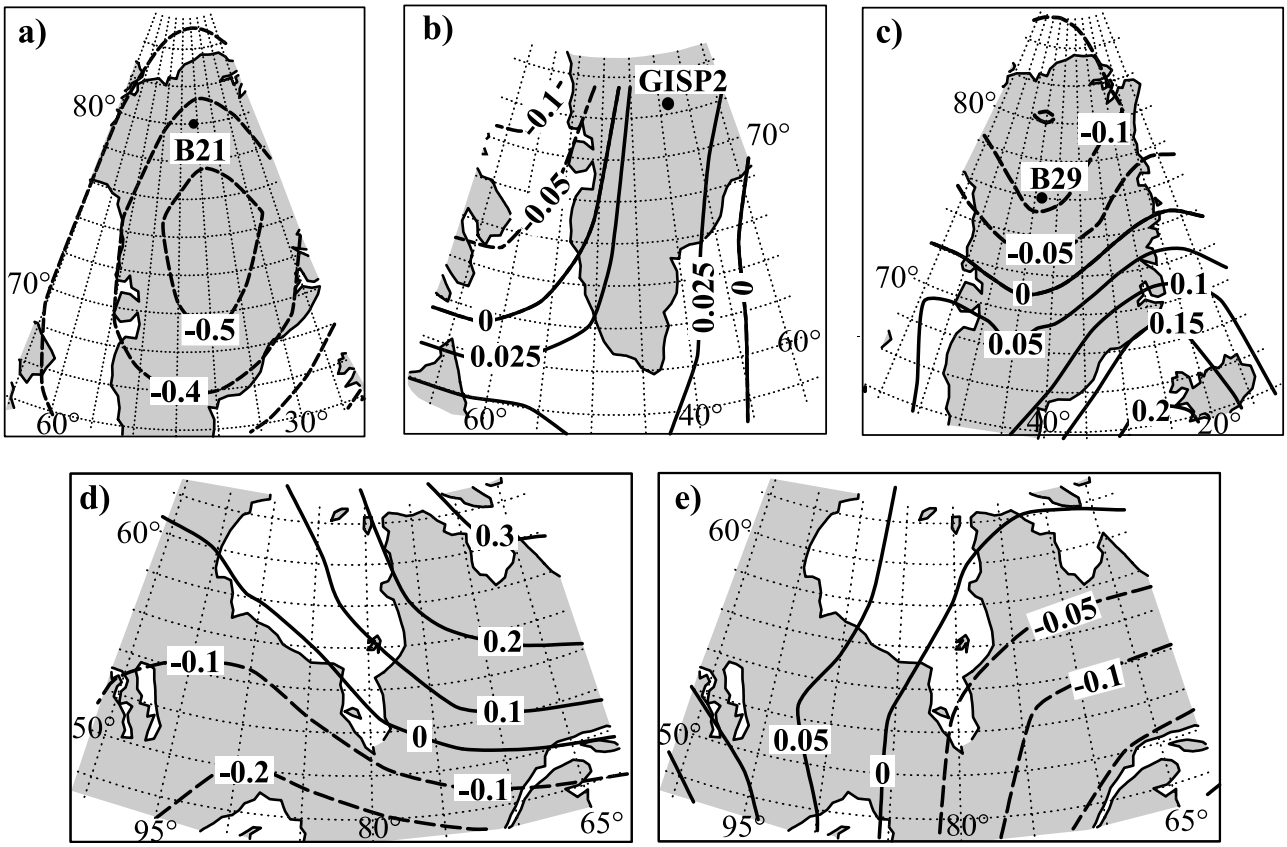


**Figure 14.** Temperature-only regression models: EOFs of 700 hPa annual temperature [°C] ((a) B21 (first EOF) [*Crüger and von Storch*, 2002]; (b) GISP2 (fourth EOF); (c) B29 (third EOF); (d) NASA-U (second EOF) and (e) NASA-U (third EOF).

models have been developed that partly relate positive ice accumulation anomalies to negative temperature anomalies. This result probably reflects the fact that these regression models do not distinguish between dynamic and thermodynamic effects, thus the temperature patterns include dynamic effects. Since the dynamic/thermodynamic regression models have shown that accumulation is mainly dynamically controlled, the patterns of the temperature models are mostly determined by circulation. The question arises as to whether the dynamic/thermodynamic regression models yield temperature patterns, representing the thermodynamically induced accumulation, that relate positive temperature anomalies to an increased accumulation. Actually, for NASA-U the temperature EOF pattern shows a pronounced maximum near the drilling site. It can be speculated that, if a considerable proportion of accumulation is thermodynamically controlled, these contributions relate positive temperature anomalies to positive accumulation anomalies. However, this could only be found for NASA-U. For the other cores, the thermodynamically described accumulation is small and possibly includes some smaller dynamic effects, which could not be attributed to stream function and hence influence the temperature patterns (see above).

## 6. Conclusions

[52] For the first time, local ice core accumulation has been directly described by means of atmospheric fields. For each investigated accumulation record we developed two kinds of regression models: one distinguishes between dynamic and thermodynamic processes by a stepwise use of stream function and temperature fields. Applying these relationships, between 56% and 73% of the multiannual accumulation variability can be explained for six of the seven records. The regression models show that the dynamics are the dominant factor for the description of accumulation. In other respects, there is no common feature found for the regression models. This leads to the conclusion that in general local accumulation only represents regional-scale information, but no large-scale climate features.

[53] Furthermore, regression models were built that only linearly relate temperature to local accumulation. Here, for five of the seven investigated cores, the explained variances amount between 48% and 57% of the multiannual accumulation variability. The main characteristics of these models also widely differ from each other. In particular, the regression models do not relate positive temperature anomalies to positive accumulation anomalies. This means that it does not seem to be feasible to derive past and future accumulation rates from isotopic temperatures. This also leads to the conclusion that it is not reasonable to apply a simple positive correlation between accumulation and temperature in mass balance models for the Greenland ice sheet. Instead of this, a more detailed description of the high spatial variability of accumulation, as performed e.g. in highly resolved General Circulation Models, should be used.

[54] **Acknowledgments.** We are grateful to the Alfred-Wegener Institute for Polar and Marine Research in Bremerhaven (Germany) for providing the ice core data. NCEP/NCAR provided the reanalysis data. Special thanks go to Beate Gardeike for preparing the figures and Julie Jones for helping with the English. This work was funded by the Helmholtz Gemeinschaft under KIHZ (Climate in Historical Times).

## References

Alley, R. B., et al. (1993), Abrupt increase in Greenland snow accumulation at the end of the Younger Dryas event, *Nature*, *362*, 527–529.

Anklin, M., R. C. Bales, E. Mosley-Thompson, and K. Steffen (1998), Annual accumulation at two sites in northwest Greenland during recent centuries, *J. Geophys. Res.*, *103*(D22), 28,775–28,783.

Appenzeller, C., J. Schwander, S. Sommer, and T. F. Stocker (1998a), The North Atlantic Oscillation and its imprint on precipitation and ice accumulation in Greenland, *Geophys. Res. Lett.*, *25*(11), 1939–1949.

Appenzeller, C., T. F. Stocker, and M. Anklin (1998b), North Atlantic Oscillation dynamics recorded in Greenland ice cores, *Science*, *282*, 446–449.

Bales, R. C., J. R. McConnell, E. Mosley-Thompson, and B. Csatho (2001), Accumulation over the Greenland ice sheet from historical and recent records, *J. Geophys. Res.*, *106*(D24), 33,813–33,825.

Briffa, K. R., T. J. Osborn, and F. H. Schweingruber (2004), Large-scale temperature inferences from tree rings: A review, *Global Planet. Change*, *40*, 11–26.

Bromwich, D. H., and F. M. Robasky (1993), Recent precipitation trends over the polar ice sheets, *Meteorol. Atmos. Phys.*, *51*, 259–274.

Charles, C. D., D. Rind, J. Jouzel, R. D. Koster, and R. G. Fairbanks (1994), Glacial-interglacial changes in moisture sources for Greenland: Influences on the ice core record of climate, *Science*, *263*, 508–511.

Chen, Q.-S., D. H. Bromwich, and L. Bai (1997), Precipitation over Greenland retrieved by a dynamic method and its relation to cyclonic activity, *J. Clim.*, *10*(5), 839–870.

Clausen, H. B., N. S. Gundestrup, S. J. Johnsen, R. Bindschadler, and J. Zwally (1988), Glaciological investigations in the Crete area, central Greenland: A search for a new deep-drilling site, *Ann. Glaciol.*, *10*, 10–15.

Crüger, T., and H. von Storch (2002), Creation of ''artificial ice core'' accumulation from large-scale GCM data: Description of the downscaling method and application to one north Greenland ice core, *Clim. Res.*, *20*, 141–151.

Cuffey, K. M., and G. D. Clow (1997), Temperature, accumulation, and ice sheet elevation in central Greenland through the last deglacial transition, *J. Geophys. Res.*, *102*(C12), 26,383–26,396.

Cuffey, K. M., G. D. Clow, R. B. Alley, M. Stuiver, E. D. Waddington, and R. W. Saltus (1995), Large Arctic temperature change at the Wisconsin-Holocene glacial transition, *Science*, *270*, 455–458. (Available at http://www.ngdc.noaa.gov/paleo/icecore/greenland/summit/)

Dahl-Jensen, D., and S. J. Johnsen (1986), Palaeotemperatures still exist in the Greenland ice sheet, *Nature*, *320*, 250–252.

Dahl-Jensen, D., S. J. Johnsen, C. U. Hammer, H. B. Clausen, and J. Jouzel (1993), Past accumulation rates derived from observed annual layers in the GRIP ice core from Summit, central Greenland, in *Ice in the Climate System*, *NATO ASI Ser. I*, vol. 12, edited by W. R. Peltier, pp. 517–532, Springer-Verlag, New York.

Dahl-Jensen, D., K. Mosegaard, N. Gundestrup, G. D. Clow, S. F. Johnsen, A. W. Hansen, and N. Balling (1998), Past temperatures directly from the Greenland Ice Sheet, *Science*, *282*, 268–271.

Dansgaard, W. (1953), The abundance of $^{18}O$ in atmospheric water and water vapor, *Tellus*, *5*, 461–469.

Dansgaard, W. (1964), Stable isotopes in precipitation, *Tellus*, *16*, 436–467.

Dansgaard, W., J. W. C. White, and S. J. Johnsen (1989), The abrupt termination of the Younger Dryas climate event, *Nature*, *339*, 532–534.

Dethloff, K., M. Schwager, J. H. Christensen, S. Kilsholm, A. Rinke, W. Dorn, F. Jung-Rothenhäusler, H. Fischer, S. Kipfstuhl, and H. Miller (2002), Recent Greenland accumulation estimated from regional climate model simulations and ice core analysis, *J. Clim.*, *15*(19), 2821–2832.

Fischer, H. (1997), Räumliche Variabilität in Eiskernzeitreihen Nordgrönlands, Ph.D. thesis, Univ. of Heidelberg, Heidelberg, Germany.

Fisher, D. A., N. Reeh, and H. B. Clausen (1985), Stratigraphic noise in time series derived from ice cores, *Ann. Glaciol.*, *7*, 76–83.

Fisher, D. A., R. M. Koerner, K. Kiuvinen, H. B. Clausen, S. J. Johnsen, J.-P. Steffensen, N. Gundestrup, and C. U. Hammer (1996), Intercomparison of ice core $\delta^{18}O$ and precipitation records from sites in Canada and Greenland over the last 3500 years and over the last few centuries in detail using EOF techniques, in *Climatic Variations and Forcing Mechanisms of the Last 2000 Years*, *NATO ASI Ser. I*, vol. 41, edited by P. D. Jones, R. S. Bradley, and J. Jouzel, pp. 297–328, Springer-Verlag, New York.

Gagan, M. K., L. K. Ayliffe, J. W. Beck, J. E. Cole, E. R. M. Druffel, R. B. Dunbar, and D. P. Schrag (2000), New Views of tropical paleoclimates from corals, *Quat. Sci. Rev.*, *19*, 45–64.

Glueck, M. F., and C. W. Stockton (2001), Reconstruction of the North Atlantic Oscillation, *Int. J. Climatol.*, *21*, 1453–1465.

Greve, R. (2000), On the response of the Greenland ice sheet to greenhouse climate change, *Clim. Change*, *46*, 289–303.

GRIP Members (1993), Climate instability during the last interglacial period record in the GRIP ice core, *Nature*, *364*, 203–207.

Hausbrand, R. (1998), Direktmessung der Azidität in einem Eisbohrkern aus Nordwestgrönland, Diplomarbeit, Univ. of Heidelberg, Heidelberg, Germany.

Huybrechts, P., and J. de Wolde (1998), The dynamic response of the Greenland and Antarctic ice sheets to multiple century climatic warming, *J. Clim.*, *12*(8), 2169–2188.

Jenkins, G. M., and D. G. Watts (1968), *Spectral Analysis and Its Applications*, Holden-Day, San Francisco, Calif.

Johnsen, S. J., H. B. Clausen, W. Dansgaard, K. Fuhrer, N. Gundestrup, C. U. Hammer, P. Iversen, J. Jouzel, B. Stauffer, and J. P. Steffensen (1992), Irregular glacial interstadials recorded in a new Greenland ice core, *Nature*, *359*, 311–313.

Johnsen, S. J., D. Dahl-Jensen, W. Dansgaard, and N. Gundestrup (1995), Greenland palaeotemperatures derived from GRIP bore hole temperature and ice core isotope profiles, *Tellus, Ser. B*, *47*, 624–629.

Jones, J. M., and M. Widmann (2003), Instrument- and tree-ring-based estimates of the Antarctic Oscillation, *J. Clim.*, *16*, 3511–3524.

Kalnay, E., et al. (1996), The NCEP/NCAR 40-Year Reanalysis Project, *Bull. Am. Meteorol. Soc.*, *77*(3), 437–471.

Kapsner, W. R., R. B. Alley, C. A. Shuman, S. Anandakrishnan, and P. M. Grootes (1995), Dominant influence of atmospheric circulation on snow accumulation in Greenland over the past 18.000 years, *Nature*, *373*, 52–54.

Kistler, R., et al. (2001), The NCEP-NCAR 50-year reanalysis: Monthly means CD-ROM and documentation, *Bull. Am. Meteorol. Soc.*, *82*(2), 247–267.

Kuhns, H., C. Davidson, J. Dibb, C. Stearns, M. Bergin, and J.-L. Jaffrezo (1997), Temporal and spatial variability of snow accumulation in central Greenland, *J. Geophys. Res.*, *102*(D25), 30,059–30,068.

McConnell, J. R., R. J. Arthern, E. Mosley-Thompson, C. H. Davis, R. C. Bales, R. Thomas, J. F. Burkhart, and J. D. Kyne (2000a), Changes in Greenland ice sheet elevation attributed primarily to snow accumulation variability, *Nature*, *406*, 877–879.

McConnell, J. R., E. Mosley-Thompson, D. H. Bromwich, R. C. Bales, and J. D. Kyne (2000b), Interannual variations of snow accumulation on the Greenland Ice Sheet (1985–1996): New observations versus model predictions, *J. Geophys. Res.*, *105*(D3), 4039–4046.

Meese, D. A., A. J. Gow, P. Grootes, P. A. Mayewski, M. Ram, M. Stuiver, K. C. Taylor, E. D. Waddington, and G. A. Zielinski (1994), The accumulation record from GISP2 core as an indicator of climate change throughout the Holocene, *Science*, *266*, 1680–1682.

Michaelson, J. (1987), Cross-validation in statistical climate forecasts models, *J. Clim. Appl. Meteorol.*, *26*, 1589–1600.

Ohmura, A., and N. Reeh (1991), New precipitation and accumulation maps for Greenland, *J. Glaciol.*, *37*(125), 140–148.

Ohmura, A., M. Wild, and L. Bengtsson (1996), A possible change in mass balance of Greenland and Antarctic ice sheets in the coming century, *J. Clim.*, *9*, 2124–2135.

Ohmura, A., P. Calanca, M. Wild, and M. Anklin (1999), Precipitation, accumulation, and mass balance of the Greenland ice sheet, *Z. Gletscherkd. Glazialgeol.*, *35*(1), 1–20.

Petit, J. R., et al. (1999), Climate and atmospheric history of the past 420.000 years from the Vostok ice core, Antarctica, *Nature*, *399*, 429–436.

Pomeroy, J. W., and H. G. Jones (1996), Wind-blown snow: Sublimation, transport, and changes to polar snow, in *Chemical Exchange Between the Atmosphere and Polar Snow*, *NATO ASI Ser. I*, vol. 43, edited by E. W. Wolff and R. C. Bales, pp. 453–489, Springer-Verlag, New York.

Schwager, M. (2000), Eisbohrkernuntersuchungen zur räumlichen und zeitlichen Variabilität von Temperatur und Niederschlagsrate im Spätholozän in Nordgrönland, *Rep. Polar Res. 362*, Alfred Wegener Inst. for Polar and Mar. Res., Bremerhaven, Germany.

Serreze, M. C., J. E. Box, R. G. Barry, and J. E. Walsh (1993), Characteristics of Arctic synoptic activity, 1952–1989, *Meteorol. Atmos. Phys.*, *51*, 147–164.

Sommer, S. (1996), Hochauflösende Spurenstoffuntersuchungen an Eisbohrkernen aus Nord-Grönland, Diplomarbeit, Univ. of Bern, Bern.

Trenberth, K. E., and D. A. Paolino (1980), The northern hemispheric sea level pressure data set: Trends, errors, and discontinuities, *Mon. Weather Rev.*, *108*, 855–872.

van der Veen, C. J., and J. F. Bolzan (1999), Interannual variability in net accumulation on the Greenland Ice Sheet: Observations and implications for mass balance measurements, *J. Geophys. Res.*, *104*(D2), 2009–2014.

van de Wal, R. S. W., M. Wild, and J. De Wolde (2001), Short-term volume changes of the Greenland ice sheet in response to doubled $CO_2$ conditions, *Tellus, Ser. B*, *53*, 94–102.

von Storch, H., and F. W. Zwiers (1999), *Statistical Analysis in Climate Research*, 1st ed., 484 pp., Cambridge Univ. Press, New York.

Washington, W. M., and C. L. Parkinson (1986), *An Introduction to Three-dimensional Climate Modeling*, 422 pp., Univ. Sci., Mill Valley, Calif.

Werner, M., U. Mikolajewicz, M. Heimann, and G. Hoffmann (2000), Borehole versus isotope temperatures on Greenland: Seasonality does matter, *Geophys. Res. Lett.*, *27*(5), 723–726.

Wild, M., and A. Ohmura (2000), Change in mass balance of polar ice sheets and sea level from high-resolution GCM simulations of greenhouse warming, *Ann. Glaciol.*, *30*, 197–203.

T. Crüger and H. von Storch, Institute for Coastal Research, GKSS Research Centre, Max-Planck-Strasse, D-21502 Geesthacht, Germany. (crueger@gkss.de)

H. Fischer, Alfred Wegener Institute for Polar and Marine Research (AWI), D-27515 Bremerhaven, Germany.